JOM, Vol. 64, No. 7, 2012
DOI: 10.1007/s11837-012-0365-6

Computational Thermodynamics Aided High-Entropy Alloy Design

CHUAN ZHANG,[1,2] FAN ZHANG,[1] SHUANGLIN CHEN,[1] and WEISHENG CAO[1]

1.—CompuTherm LLC, 437 S. Yellowstone Dr., Suite 217, Madison, WI 53719, USA. 2.—e-mail: Chuan.Zhang@computherm.com

Thermodynamic calculation is used to shed light on the design and development of high-entropy alloys (HEAs) in this article. A thermodynamic database for the Al-Co-Cr-Fe-Ni was developed, and phase diagrams of this system were calculated. The calculated results, such as primary solidified phases, which are fractions of stable phases at a given alloy composition, explain the published experimental observations fairly well for both as-cast and homogenized alloys. These calculations also confirm the effect of each element on the face-centered cubic (fcc)/body-centered cubic (bcc) structure transition as published in the literature. The role of thermodynamic calculation in aiding effective design of HEAs is clearly demonstrated by this work.

INTRODUCTION

High-entropy alloy (HEA), representing a new concept of alloy design, has revolutionized the traditional alloy design approach, which is usually based on one or, at most two key elements. On the contrary, HEAs have multiprincipal elements that are in equal, or near to equal, atomic ratios. Surprisingly, rather than forming the anticipated complex microstructure with a mixture of compounds, HEA tends to form a simple solid solution structure, such as face-centered cubic (fcc) or body-centered cubic (bcc), or a mixture of both. This tendency is due to the high entropy of mixing of the solution phases. Thermodynamically, a system reaches equilibrium when the Gibbs energy of the system reaches its global minimum at constant temperature and pressure. The Gibbs energy of mixing of a solution phase is described as

$$\Delta G_{\mathrm{mix}} = \Delta H_{\mathrm{mix}} - T\Delta S_{\mathrm{mix}} \quad (1)$$

In which ΔH_{mix} is the enthalpy of mixing and ΔS_{mix} is the entropy of mixing. For a random mixing of components, the configurational entropy of mixing is calculated by

$$\Delta S_{\mathrm{mix}} = -\mathrm{R}\sum_{i=1}^{n} x_i \ln(x_i) \quad (2)$$

T is the temperature in Kelvin and R is the gas constant. For an n-element solution phase, the ΔS_{mix} reaches its maximum $Rln(n)$, when an equal molar fraction of each element (x_i) is used. A higher entropy of mixing leads to lower Gibbs energy at constant temperature, which makes the solution phase tend to be more stable.[1,2]

HEAs have attracted more and more attention in recent years due to their numerous beneficial mechanical, magnetic, and electrochemical characteristics, such as high strength, high thermal stability, high wear resistance, and high oxidation resistance. These promising properties offer many potential applications in various fields, such as tools, molds, dies, diffusion barriers, and soft magnetic films.[1,3–6] Current research on HEAs mostly focuses on the AlxCoCrCuFeNi alloys, while the addition of other components such as Ti and Mn are also explored.[7–15] It is found that the addition of Al and other elements has a strong effect on the properties of the HEAs. For example, the structure of the Al$_x$CoCrFeNi alloys varies from fcc to fcc + bcc and to fully bcc[5,16,17] with the increasing of Al ratio. The hardness and strength increase with the increasing amount of the bcc phase, but the alloy becomes more brittle.[18,19] Many publications have focused on understanding and controlling the structures within the as-cast and/or homogenized HEAs.

(Published online June 29, 2012)

Even though HEAs are based on the concept of multiprincipal elements, it does not mean that one can develop HEAs by simply mixing a bunch of elements together with an equal atomic ratio. Now the question is how to select the principal elements with proper ratios so that HEAs with desired properties can be developed. Up to now, a tremendous amount of effort has been made on the investigation of the fcc/bcc phase transition of the HEAs with the addition of different alloying elements. In addition to use the traditional trial and error method, several criteria have been proposed in the literature.[20] These criteria include the following:

- High entropy of mixing ($\Delta S_{mix} > 1.61R$), which requires at least five principal components in the system with equal atomic ratio.
- Small enthalpy of mixing ($-15 < \Delta_{mix} < 5$ kJ/mol), which is due to the fact that a large positive enthalpy of mixing results in the segregation of different elements, and a large negative enthalpy of mixing leads to the formation of compounds.
- Small atomic size difference ($\delta < 4.6$), which favors the formation of solid-solution phase.

Recently, the effect of valence electron concentration on the stability of fcc/bcc phase in the HEAs was discussed by Guo et al.[21] and the (bcc) $6.87 \leq \mathrm{VEC} = \sum_{i=1}^{n} c_i(\mathrm{VEC})_i < 8$(fcc) criterion was proposed on the basis of the experimental data of the $Al_xCoCrCuFe$, $Al_xCrCuFeNi_2$ and $Al_xCoCrCuFeNi$ systems.

However, the above criteria derived from certain series of experimental data are system dependent and may not be applicable to other systems. It, therefore, needs an alternative approach that can be used to guide the selection of suitable elements and compositions for the development of HEAs with desired properties. According to thermodynamics, the equilibrium state and the developed microstructure of an alloy is a result of stability competition among all the phases in a system. Phase diagrams, which are graphic representation of phase relationship in a system, provide detailed information on the stability of phases as a function of composition, temperature, and pressure. They are, therefore, the road maps for materials scientists/engineers in alloy design and development. Phase diagrams have been traditionally determined purely by experimentation, which is costly and time consuming. While an experimental approach is feasible for the determination of binary and simple ternary phase diagrams, it is less efficient for the complicated ternaries and becomes extremely challenging for higher order systems over wide ranges of composition and temperature. On the other hand, commercial alloys are often multicomponents in nature, and HEAs usually require at least five components. In order to understand the phase relationship in the HEA systems, a more efficient approach is therefore needed in the determination of multicomponent phase diagrams. In recent years, a phenomenological approach, or the CALPHAD approach,[22] has been widely used for the study of phase equilibria of multicomponent systems. In this approach, separately measured phase equilibrium data and thermodynamic properties are converted to a unique thermodynamic description of the system in question. This thermodynamic description can be used not only to reproduce the known thermodynamic properties but also to predict the unknown thermodynamic properties of the system. More importantly, thermodynamic descriptions of the constituent binaries and ternaries can be combined and extrapolated on the basis of geometric models to develop a thermodynamic description of a multicomponent system. The term "thermodynamic database" or "database" is usually used for a multicomponent system instead of "thermodynamic description." The ultimate goal of the CALPHAD approach is to use the thermodynamic database developed to predict phase equilibria and thermodynamic properties of a multicomponent system that are usually not experimentally available. The application of the CALPHAD approach in aiding materials design has been discussed elsewhere.[23–25] Especially, this approach has been successfully used to predict the forming ability of metastable bulk metallic glasses.[26–29] In this study, this approach is used to predict the fcc/bcc phase transition of both as-cast and homogenized AlxCoCrFeNi HEAs. The calculated results are compared with the available literature data.

CALCULATION AND DISCUSSION

A thermodynamic database for the Al-Co-Cr-Fe-Ni was developed using the CALPHAD approach, and phase diagrams were calculated to understand the phase relationships in this system. The current Al-Co-Cr-Fe-Ni database was obtained via extrapolation from the lower order constituent binary and ternary systems at the whole composition range. Based on our experience,[23–29] the interaction parameters of lower order constituent systems are the most effective and important to obtain a reliable higher order thermodynamic database. Note that no higher order (quaternary or quinary) interaction parameters were used in our current thermodynamic database. Some ternary phases were modeled in our current thermodynamic database on the basis of the literature experimental data. No higher order phases (quaternary or quinary) have been reported in the literature. All calculations throughout this paper are carried out by Pandat[30] software (CompuTherm LLC, Madison, WI). Figure 1 shows the vertical section of the CoCrFeNi-AlxCoCrFeNi with x varies between 0 and 3. This figure clearly demonstrates the phase stability change when adding Al to the CoCrFeNi alloy. It is seen that when $x < 0.75$, the primary solidified phase is fcc, and when $x > 0.75$, it is bcc_$B2$, which solidifies first. In the following, we will use bcc_$A2$ to represent the

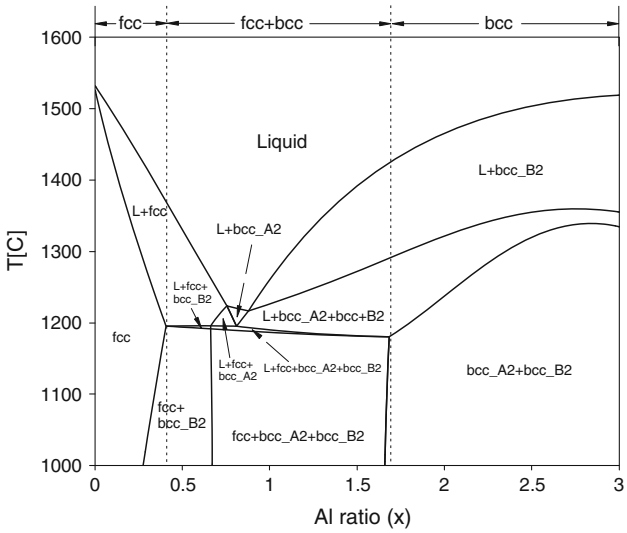

Fig. 1. The calculated isopleth of the $Al_xCoCrFeNi$ alloys with x = 0–3 using our current thermodynamic description.

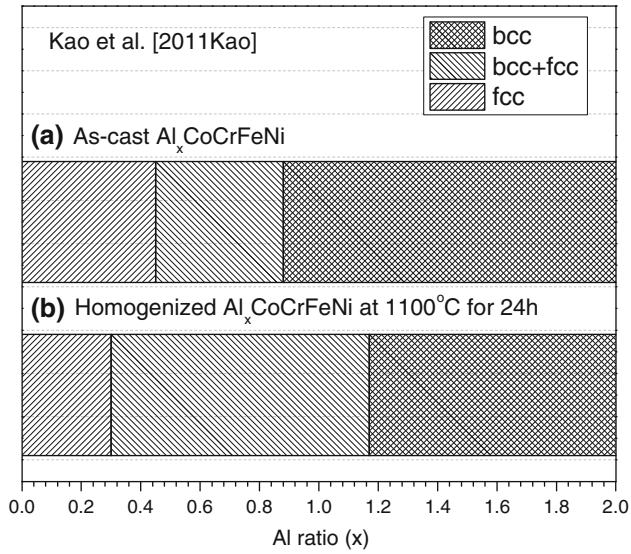

Fig. 2. Experimentally measured transition ranges of the $Al_xCoCrFeNi$ alloys by Kao et al.[34]: (a) as-cast and (b) homogenized at 1100°C for 24 h.

disordered bcc structure and bcc_*B*2 to represent the ordered structure, both of which exist in this system. If bcc is used, then it means bcc structure in general, either ordered or disordered or the mixture of both. Figure 1 indicates that pure fcc structure will be developed if a small *A*l ratio is used, while the bcc structure will be developed if a higher Al ratio is used, and a mixture of fcc + bcc should be seen in between. This is exactly what was observed by many researchers who have carried out experimental studies of Al*x*CoCrFeNi alloys.[7,12,16,31–34]

Recently, Kao et al.[34] conducted systematic microstructure investigations on the as-cast, homogenized, and deformed $Al_xCoCrFeNi$ HEAs with various Al contents. Figure 2 shows their experimental observation of microstructure dependence on the Al content for both as-cast and homogenized conditions. As is shown in Fig. 2a for the as-cast structure, they found that it is an fcc structure when $x < 0.45$ and a bcc structure when $x > 0.88$. The fcc + bcc duplex structure was seen when the Al ratio is in the midrange, i.e., $0.45 < x < 0.88$. Since the as-cast structure is developed with a very high cooling rate, Scheil simulation is carried out in this study to explain the structures obtained by Kao et al.[34] Figure 3 shows the Scheil simulation of fraction of solid as a function of temperature for various Al ratios. Figure 3a, shows an fcc + bcc structure solidified together from liquid even for $x = 0.1$. However, with this small Al ratio, 99.2% of the liquid forms the primary fcc phase, and the total amount of bcc formed from the calculation is only 0.23%, which is hardly seen even though it does exist. When $x = 0.3$, even though 10% of the liquid is left after primary solidification of fcc phase, the total bcc phase that may form is only 2.3% according to the calculation. It is not surprising that no bcc was observed by Kao et al.[34] when $x = 0.3$. The structure starts to change for the case of $x = 0.5$. It is seen from Fig. 3a that 35% liquid is still there to form fcc + bcc duplex structure when $x = 0.5$. The simulation shows that the total bcc that may form in this case is 7.4%, which is sufficient to be observed in the microstructure. The simulation for $x = 0.8$ shows very interesting features. The primary solidified phase is bcc-*B*2 (total 2.4%), while 97.6% liquid forms the mixture of bcc_*B*2 + bcc_*A*2 + fcc. The solidification of this alloy finishes in a narrow temperature range, from 1263°C to 1191°C. This composition is close to the so-called deep eutectic point and may develop into an amorphous structure.[35]

Figure 3b shows the solidification curves for $x \geq 0.8$ of the $Al_xCoCrFeNi$ alloys, which indicate that the primary solidified phase is bcc_*B*2. Even though Kao et al.[34] observed only bcc structure for $x > 0.88$, many publications suggested that this is true only when $x > 1.0$.[16,17,36] According to our simulation as shown in Fig. 3b, when $x = 1.0$, only 7% of the liquid is consumed to form the primary bcc_*B*2 and the next 20% of liquid forms bcc phases (both bcc_*A*2 and bcc_*B*2). Then, the rest of liquid forms bcc + fcc structures. What should be mentioned is that the temperature only drops less than 15°C (1189–1175°C) for the bcc + fcc mixture to finish solidification. It should also be pointed out that the simulation shows that the bcc structure is a mixture of ordered bcc-*B*2 and disordered bcc_*A*2 when $x > 1.0$, which is consistent with many published experimental works.[16,17,36] The simulation shows that the fcc phase should appear even when $x = 2$, while in reality, one may not observe it due to its insignificant amount. As is seen, with the increasing of x, the amount of liquid left for the $L \rightarrow$ bcc_*B*2 + bcc_*A*2 + fcc reaction becomes

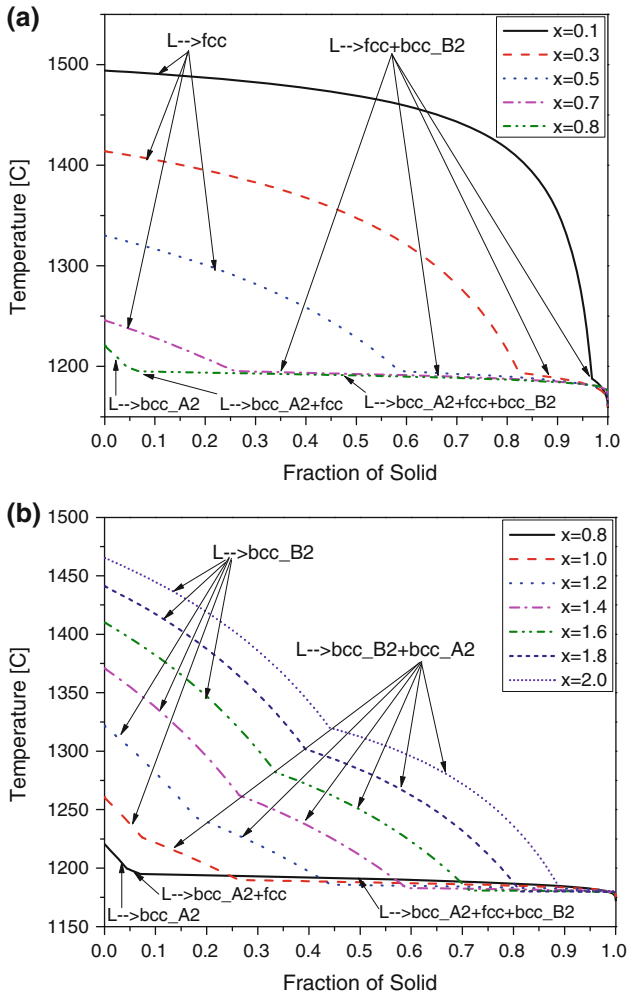

Fig. 3. Solidification paths calculated by the Scheil model for the $Al_xCoCrFeNi$ alloys using our current thermodynamic database: (a) x = 0.1–0.8 and (b) x = 0.8–2.0.

smaller, and the solidification temperature range gets smaller. Both factors make it difficult to see the fcc phase in the solidified microstructure under a high cooling rate.

In addition to the as-cast structure, Kao et al.[34] also characterized the structure evolution of the homogenized $Al_xCoCrFeNi$ HEAs at 1100°C for 24 h. Their experimental data indicated that the fcc + bcc transition region is at $0.3 < x < 1.17$, which agrees with the calculated phase boundary ($0.35 < x < 1.34$) of this study fairly well (Fig. 1). Note that the calculated phase diagram corresponds to the equilibrium state, while the measured one may not yet reach equilibrium due to the sluggish diffusion of elements in the HEAs and short annealing period (24 h). Chou et al.[16] also investigated the phase transformation of $Al_xCoCrFeNi$ alloys at low temperatures using the differential thermal analysis (DTA) (<1200 K) and high-temperature x-ray diffraction (HTXRD) (<1000 K). The precipitation of a σ phase that has a NiCoCr structure was found at temperatures higher than 873 K.

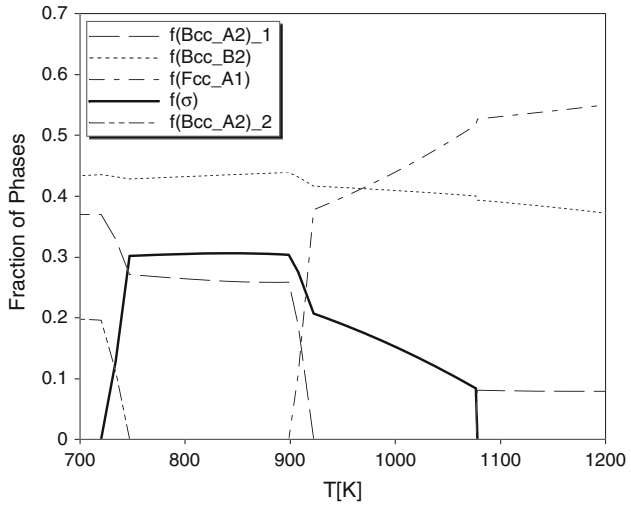

Fig. 4. Equilibrium calculation of phase fraction as a function of temperature for the $Al_{0.875}CoCrFeNi$ alloy using our current thermodynamic database.

Using the thermodynamic database we developed in this study, an equilibrium line calculation is performed for the $Al_{0.875}CoCrFeNi$ alloy. As shown in Fig. 4, the σ phase does form in the temperature range of 720 K to 1078 K. Chou et al.[16] did not observe the σ phase between 720 K and 873 K, which is not surprising. Since the precipitation is a diffusion-controlled process and a certain amount of phase is necessary for the HTXRD phase identification, the observed precipitation of a σ phase will be delayed during both the DTA and the HTXRD measurements. Excluding the uncertainties from both experimentation and thermodynamic calculation, our thermodynamic prediction shown in Fig. 4 agrees qualitatively with the experimental observation of Chou et al.[16] Further systematic phase transformation study for the $Al_xCoCrFeNi$ alloys will be necessary especially in the solid state for quantitative comparison.

It has been found that both Al and Cr are stabilizers of the bcc-based structure.[36,37] The effect of Al on the fcc/bcc phase transition has been discussed above in detail. It will be interesting to understand the effect of Cr in this regard. To take advantage of thermodynamic calculation, the isopleths of $AlCoCr_yFeNi$-Al_xCoCr_yFeNi with y = 0.5, 1, 1.5, and 2, respectively, were calculated and shown in Fig. 5a–d. With the increasing addition of Cr ratios from 0.5 to 2 as shown in Fig. 5a–d, the disordered bcc-$A2$ phase becomes stable in larger and larger composition and temperature ranges at the expense of both ordered bcc_$B2$ and fcc. Figure 4 clearly indicates the difference of Al and Cr. In general, Al stabilizes both bcc_$A2$ and bcc_$B2$, yet it is more in favor of bcc_$B2$, while Cr stabilizes bcc_$A2$ but destabilizes bcc_$B2$. The phase transition ranges of Al_xCoCr_yFeNi alloys homogenized at 1100°C were also calculated and shown in Fig. 6. It indicates the bcc phase region increases and the fcc/fcc + bcc regions

decrease with the increasing of Cr concentration. When the Cr ratio x = 2.0, no pure fcc phase region can form within the Al_xCoCr_2FeNi alloys.

Isopleths with various ratios of Co, Fe, and Ni are also calculated in order to fully understand the effect of each element on the fcc/bcc phase transition of the AlCoCrFeNi-based HEAs. Figure 7a is the vertical section of AlCrFeNi-AlCoxCrFeNi, Fig. 7b is the vertical section of AlCoCrNi-AlCoCrFexNi, and Fig. 7c is that for the AlCoCrFe-AlCoCrFeNix. As is seen from Fig. 7, the Co, Fe, and Ni all act as fcc stabilizers. On the other hand, it is hard to get an fcc structure as the primary phase in all three vertical sections. This is because high Al ratio (Al = 1) is used in the calculation of these diagrams.

It should be pointed out that most of the HEAs were prepared by arc melting and then drop casting, which maintain the structure of the primary solidified phase. However, if the alloy is annealed at an elevated temperature for some time, a second or even third phase may precipitate from the matrix phase. The final structure of the alloy depends on the alloy chemistry and heat treatment temperature. The phase stability at different temperatures and compositions can be found from phase diagrams, such as those shown in Figs. 1, 5, and 7.

SUMMARY

HEAs based on the Al-Co-Cr-Fe-Ni system were discussed in this study by the aid of thermodynamic

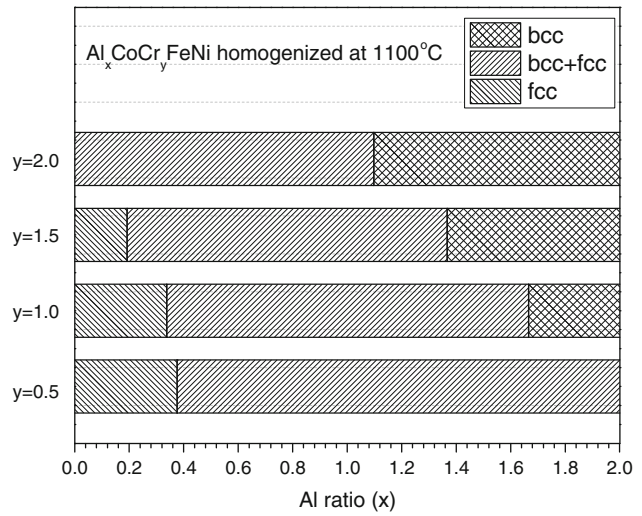

Fig. 6. The calculated transition ranges of the Al_xCoCr_yFeNi alloys homogenized at 1100°C.

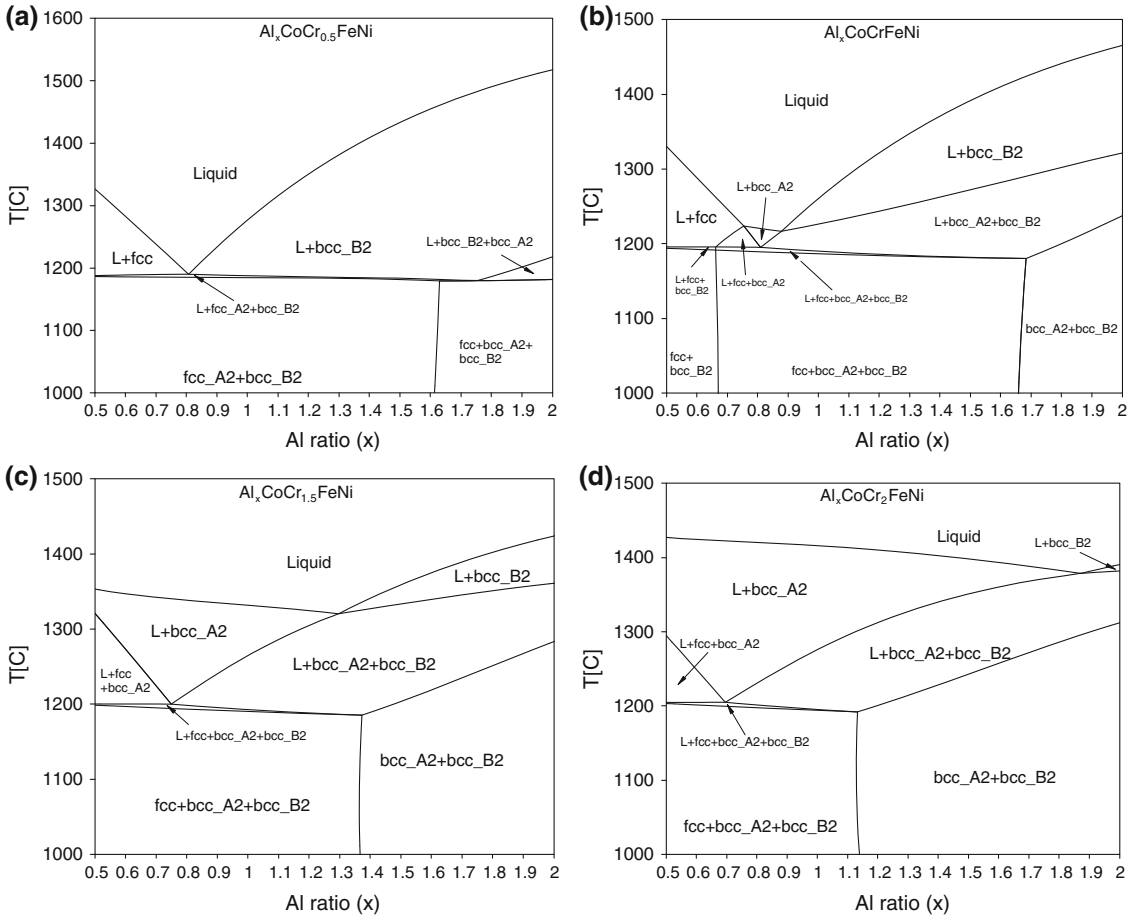

Fig. 5. The calculated isopleth of the Al_xCoCr_yFeNi alloys with x = 0.5–2, y = 0.5, 1.0, 1.5, and 2.0 using our current thermodynamic description.

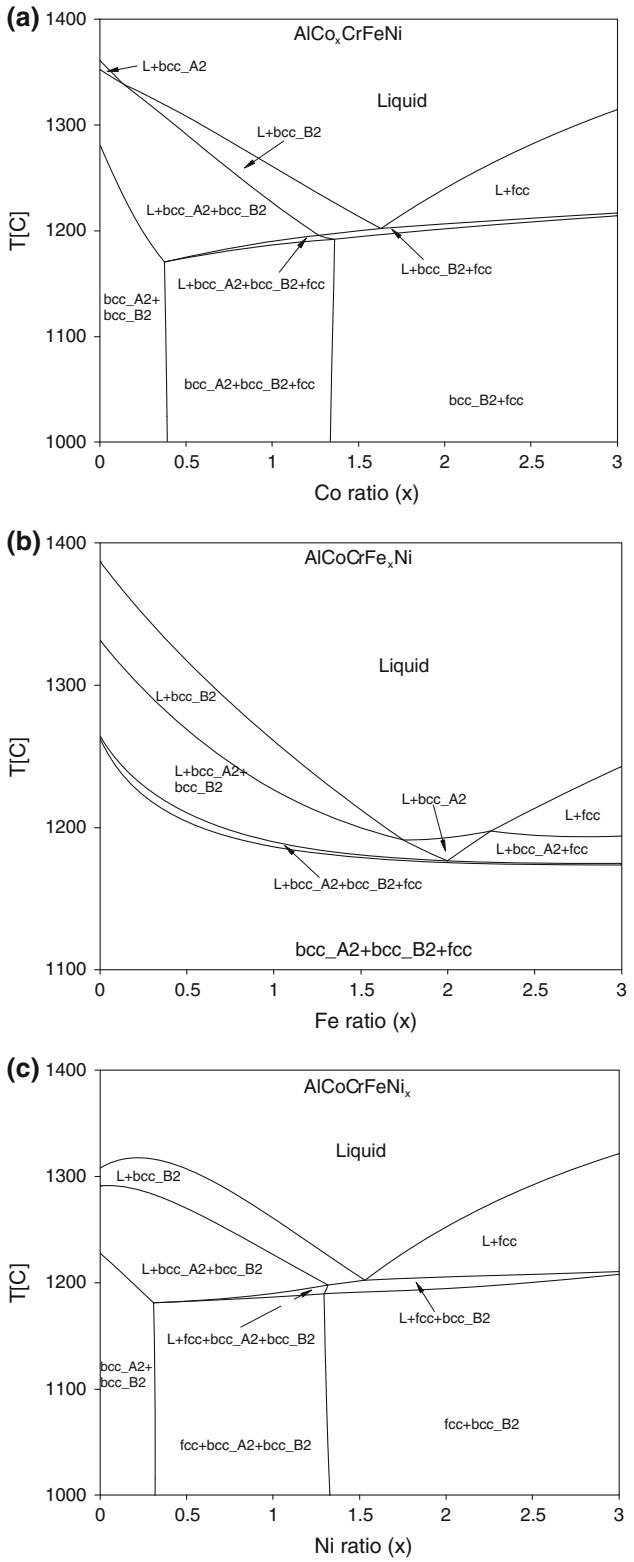

Fig. 7. The calculated isopleths of the Al-Co-Cr-Fe-Ni alloys using our current thermodynamic description with different Co, Fe, and Ni ratios, respectively.

calculation. The thermodynamic database of this system was developed, and phase diagrams and solidification curves were calculated. The calculated results explain the published experimental observations fairly well for both as-cast and homogenized alloys. In particular, the following conclusions are obtained:

- Al is found to stabilize both the disordered bcc_*A*2 and ordered bcc_*B*2 structure, and the latter is favored. To develop HEAs with a single fcc structure, a very small Al ratio ($x < 0.3$) should be used.
- Cr stabilizes the bcc_*A*2 structure and destabilizes both bcc_*B*2 and fcc structures in the AlCoCrFeNi-based HEAs.
- Co, Fe, and Ni are all fcc stabilizers, while the Al ratio must be small in order to obtain pure fcc HEAs.

This work demonstrates that thermodynamic calculations may play a key role in aiding the effective design of HEAs. These calculations can be used to understand the effect of each element on the phase stability and the fcc/bcc phase transition, and therefore, they provide us with useful guidelines in the development of HEAs. It is understood that the HEA structures can be controlled through adjusting the ratios of one or more elements. The merit of the computational approach is that virtual experiments can be carried out easily for the multicomponent system once the thermodynamic database is developed.

REFERENCES

1. J.W. Yeh, S.K. Chen, S.J. Lin, J.Y. Gan, T.S. Chin, T.T. Shun, C.H. Tsau, and S.Y. Chang, *Adv. Eng. Mater.* 6, 299 (2004).
2. J.W. Yeh, Y.L. Chen, S.J. Lin, and S.K. Chen, *Mater. Sci. Forum* 560, 1 (2007).
3. P.K. Huang, J.W. Yeh, T.T. Shun, and S.K. Chen, *Adv. Eng. Mater.* 6, 74 (2004).
4. B. Cantor, I.T.H. Chang, P. Knight, and A.J.B. Vincent, *Mater. Sci. Eng. A* 375, 213 (2004).
5. C.J. Tong, Y.L. Chen, S.K. Chen, J.W. Yeh, T.T. Shun, C.H. Tsau, S.J. Lin, and S.Y. Chang, *Metall. Mater. Trans. A* 36A, 881 (2005).
6. U.S. Hsu, U.D. Hung, J.W. Yeh, S.K. Chen, Y.S. Huang, and C.C. Yang, *Mater. Sci. Eng. A* 406, 403 (2007).
7. G.Y. Ke, S.K. Chen, T. Hsu, and J.W. Yeh, *Ann. Chim. Sci. Mater.* 31, 669 (2006).
8. P. Lee, Y.Y. Chen, C.Y. Hsu, J.W. Yeh, and H.C. Shih, *J. Electrochem. Soc.* 154, C424 (2007).
9. Y.J. Zhou, Y. Zhang, Y.L. Wang, and G.L. Chen, *Appl. Phys. Lett.* 90, 181904 (2007).
10. Y.J. Zhou, Y. Zhang, Y.L. Wang, and G.L. Chen, *Mater. Sci. Eng. A* 454, 260 (2007).
11. S. Varalakshmi, M. Kamaraj, and B.S. Murty, *J. Alloys Compd.* 460, 253 (2008).
12. Y.P. Wang, B.S. Li, M.X. Ren, C. Yang, and H.Z. Fu, *Mater. Sci. Eng. A Struct.* 491, 154 (2008).
13. S.T. Chen, W.Y. Tang, Y.F. Kuo, S.Y. Chen, C.H. Tasu, T.T. Shun, and J.W. Yeh, *Mater. Sci. Eng. A* 527, 5818 (2010).
14. K.B. Zhang and Z.Y. Fu, *Intermetallics* 22, 24 (2012).
15. S. Praveen, B.S. Murty, and R.S. Kottada, *Mater. Sci. Eng. A* 534, 83 (2012).
16. H.P. Chou, Y.S. Chang, S.K. Chen, and J.W. Yeh, *Mater. Sci. Eng. B* 163, 184 (2009).
17. Y.F. Kao, T.J. Chen, S.K. Chen, and J.W. Yeh, *J. Alloy Compd.* 488, 57 (2009).
18. C.J. Tong, M.R. Chen, S.K. Chen, J.W. Yeh, T.T. Shun, S.J. Lin, and S.Y. Chang, *Metall. Mater. Trans. A* 36A, 1263 (2005).

19. C.W. Tsai, M.H. Tsai, J.W. Yeh, and C.C. Yang, *J. Alloy Compd.* 490, 160 (2010).
20. Y. Zhang and Y.J. Zhou, *Mater. Sci. Forum* 561–565, 1337 (2007).
21. S. Guo, C. Ng, J. Lu, and C.T. Liu, *J. Appl. Phys.* 109, 103505 (2011).
22. L. Kaufman and H. Bernstein, *Computer Calculation of Phase Diagrams* (New York: Academic Press, 1970).
23. C. Zhang, H.B. Cao, V. Firouzdor, S. Kou, and Y.A. Chang, *Intermetallics* 18, 1597 (2010).
24. C. Zhang, F. Zhang, S.-L. Chen, W.-S. Cao, and Y.A. Chang, *Acta Mater.* 59, 6246 (2011).
25. F. Zhang, Y. Yang, W.S. Cao, S.L. Chen, K.S. Wu, and Y.A. Chang, *ASM Handbook on Metals Process Simulation*, Vol. 22B, ed. D.U. Furrer and S.L. Semiatin (Materials Park, OH: ASM International, 2010), p. 117.
26. H.B. Cao, D. Ma, K.C. Hsieh, L. Ding, W.G. Stratton, P.M. Voyles, Y. Pan, M.D. Cai, J.T. Dickinson, and Y.A. Chang, *Acta Mater.* 54, 2975 (2006).
27. D. Ma, H.B. Cao, and Y.A. Chang, *Intermetallics* 15, 1122 (2007).
28. H.B. Cao, Y. Pan, L. Ding, C. Zhang, J. Zhu, K.C. Hsieh, and Y.A. Chang, *Acta Mater.* 56, 2032 (2008).
29. Y. Pan, H. Cao, L. Ding, C. Zhang, and Y.A. Chang, *J. Non-Cryst. Solids* 356, 2168 (2010).
30. Pandat 8.0, *Phase Diagram Calculation Software for Multi-Component Systems* (Madison, WI: CompuTherm LLC, 2008).
31. C.M. Lin and H.L. Tsai, *Intermetallics* 19, 288 (2011).
32. H.B. Cui, Y. Wang, J.Y. Wang, X.F. Guo, and H.Z. Fu, *China Foundry* 8, 259 (2011).
33. T.T. Shun and Y.C. Du, *J. Alloy Compd.* 479, 153 (2009).
34. Y.F. Kao, S.K. Chen, T.J. Chen, P.C. Chu, J.W. Yeh, and S.J. Lin, *J. Alloy Compd.* 509, 1607 (2011).
35. Y.A. Chang, *Metall. Trans. B* 37B, 7 (2006).
36. C. Li, M. Zhao, J.C. Li, and Q. Jiang, *J. Appl. Phys.* 104, 113504 (2008).
37. C.T. Tung, J.W. Yeh, T.T. Shun, S.K. Chen, Y.S. Huang, and H.C. Cheng, *Mater. Lett.* 61, 1 (2007).